IEEE Access
Multidisciplinary | Rapid Review | Open Access Journal

Received January 20, 2022, accepted February 15, 2022, date of publication February 24, 2022, date of current version March 4, 2022.

Digital Object Identifier 10.1109/ACCESS.2022.3154111

Implementations of Full State Feedback Robust Control Designs for Mechanical Systems Using Only Positions or Velocities Output Feedback

LUCAS M. ESTEVES[1], RODRIGO CARDIM[1], MARCELO C. M. TEIXEIRA[1], (Member, IEEE), DIOGO R. DE OLIVEIRA[2], JEAN M. DE S. RIBEIRO[1], EDVALDO ASSUNÇÃO[1], AND HYAGO R. M. SILVA[1]

[1]Department of Electrical Engineering, UNESP—São Paulo State University, Ilha Solteira, São Paulo 15385-000, Brazil
[2]IFMS—Federal Institute of Education, Science and Technology of Mato Grosso do Sul, Três Lagoas, Mato Grosso do Sul 79641-162, Brazil

Corresponding author: Rodrigo Cardim (rodrigo.cardim@unesp.br)

This study was supported in part by the Coordenação de Aperfeiçoamento de Pessoal de Nível Superior - Brasil (CAPES) - Finance Code 001, São Paulo Research Foundation (FAPESP) (grant. 2011/17610-0) and Conselho Nacional de Desenvolvimento Cientifico e Tecnológico (CNPq).

ABSTRACT This paper proposes a new design and practical implementation of a robust $\mathcal{H}_\infty$ control applied to some mechanical systems considering in the controller design full access to the state variables and in the equivalent controller implementation only the feedback of all positions or of all velocities of the plant. An important characteristic, though, is that limitations are considered for the state feedback. Two methods are presented, one that uses feedback only from state variables related to positions of the system and another that uses feedback only from state variables related to velocities. The control strategy is based on Linear Matrix Inequalities (LMIs), using the theory of $\mathcal{D}$-stability, which allows the designer to allocate the closed loop system eigenvalues in a negative complex semi-plane region, which, in addition to ensuring stability, also allows to attend certain performance requirements of the feedback system. The paper motivation is to provide satisfactory control results with limited states access, without any kind of estimation of the state variables that are not available. Therefore, the proposed control systems are interesting options as alternatives for the design of full-order state feedback for plants with uncertain parameters using only output feedback, considering that it is not required to build an observer to estimate any plant state variable. Furthermore, their implementations are relatively cheaper because it is not necessary to measure all state variables of the plant.

INDEX TERMS Control system, linear matrix inequalities (LMIs), robust control, active suspension, mechanical systems, position feedback, velocity feedback.

I. INTRODUCTION

Stability analysis and the design of linear system controllers are widely explored research areas. It is a field with countless options of control techniques. Some of them use a Lyapunov function along with linear matrix inequalities (LMIs) to guarantee the stability of the system. Examples of the main advantages of using LMIs in this type of project are the easy insertion of performance indexes in the addressed system and the fact that LMIs can be solved efficiently in microcomputers using well-known softwares, as shown in [1].

Often access to all state variables of a system is a problem. In some cases one way to overcome this issue is to use some form of estimation of these state variables that are difficult to reach. It is known that this estimation becomes more difficult when the plant has uncertain parameters. However, another very interesting alternative is the implementation of a control technique that does not depend on all the states of the system. In many cases of mechanical systems, the velocity vector is difficult to access, while in other cases the issue is having access to position parameters. The solution of this problem may be of great importance on the design and implementation of control for this class of systems. A method for controlling uncertain mechanical systems, where there is no need to measure speeds, for example, could make implementations cheaper, which is highly valued.

In [2] there is a study on the nonlinear position control for permanent magnet stepper motor using only position

The associate editor coordinating the review of this manuscript and approving it for publication was Juntao Fei.

feedback, since in industrial applications the velocity measurement has been not widely used due to either its resolution or cost concern. In [3] the authors present a control of velocity for DC Motors measuring only angular position. Avila-Becerril designed in [4] a dynamic controller which is based on measurements of link and joint positions only, for flexible-joint robots. Also working with robots, [5] develops an adaptive locomotion control of hexapod walking robot for traversing rough terrains with position feedback only. A FAT (function approximation technique)-based adaptive controller is proposed in [6] for robot manipulators with position measurements only. Salam shows in [7] a method where only velocity feedback is needed to achieve position-to-position control for robot manipulators. A study that investigates the robust quantised $\mathcal{H}_\infty$ control problem for active suspension systems is presented in [8], while a different approach is taken by [9], where a fault-tolerant control approach is proposed to deal with the problem of fault accommodation for unknown actuator failures of active suspension systems. [10] presents an interesting procedure, where an output feedback controller is designed for trajectory tracking of robot manipulators without velocity measurements nor observers.

This paper proposes a new design and practical implementation of two robust $\mathcal{H}_\infty$ control methods applied to a system of active suspension manufactured by Quanser [11]. Although the designs consider access to all plant state variables, the implementations use only the feedback of all positions or of all velocities of the system. On the first method, the state feedback is composed only by state variables related to positions of the implemented system, while the second method considers the use of velocity feedback only. There is no estimate of state variables in any of the methods presented. Therefore, the proposed control systems are interesting options as alternatives for the design of full-order state feedback for plants with uncertain parameters using only output feedback, considering that it is not required to build an observer to estimate any plant state variable. Furthermore, they are relatively cheaper because it is not necessary to measure all state variables of the plant.

The software MatLab, the Yalmip language [12] and the LMILab solver were used in order to carry out the control design applying LMIs, wich were implemented using the theory of $\mathcal{D}$-stability. The main goal os this paper is to show that, even with a limited state feedback access (a particular output feedback), it is possible to obtain a satisfactory control performance. After a complete theoretical analyses of the proposed results, the effectiveness of these procedures was illustrated in the implementation of the controllers for an inverted pendulum system and for an active suspension system.

Throughout the text the following notations are used: "$(\ldots)^{\mathrm{T}}$" indicates the transposition of a vector or matrix. The symbol "$*$" generically denotes each symmetric element. $He\{.\}$ is the hermitian operator such that $He\{A\} = A + A^T$. $\|.\|_2$ represents the Euclidean norm. Lastly, $\mathscr{L}_2$ represents the set of all trajectories, such that $\|\xi\|_2^2 < \infty$.

II. ROBUST $\mathcal{H}_\infty$ CONTROL AND $\mathcal{D}$-STABILITY

Many classical control objectives can be expressed in terms of $\mathcal{H}_\infty$ performance and tackled by $\mathcal{H}_\infty$-synthesis techniques. Since it only involves solving two Riccati equations, $\mathcal{H}_\infty$ synthesis has a low complexity comparable to some other techniques. However, its design deals mostly with frequency-domain aspects and provides little control over the transient behavior and closed-loop pole location. In contrast, satisfactory time response and closed-loop damping can often be achieved by forcing the closed-loop poles into a suitable subregion of the left-half plane. In addition, fast controller dynamics can be prevented by prohibiting large closed-loop poles (often desirable for digital implementation). One way of simultaneously tuning the $\mathcal{H}_\infty$ performance and transient behavior is therefore to combine the $\mathcal{H}_\infty$ and pole-placement objectives [13].

It is well known that $\mathcal{H}_\infty$ synthesis can be formulated as a convex optimization problem involving LMIs. Because LMIs intrinsically reflect constraints rather than optimality, they tend to offer more flexibility for combining several constraints on the closed-loop system [13].

Consider the uncertain linear time-invariant system, described in the form of state variables:

$$\dot{x}(t) = A(\beta)x(t) + B(\beta)u(t) + H(\beta)w(t), \tag{1}$$
$$y(t) = C(\beta)x(t) + D(\beta)u(t) + G(\beta)w(t), \tag{2}$$

where $x(t) \in \mathbb{R}^n$ is the state vector, $u(t) \in \mathbb{R}^m$ is the controlled input, $w(t) \in \mathbb{R}^p$ is the limited exogenous input, $y(t) \in \mathbb{R}^q$ is the controlled output, $A(\beta)$, $B(\beta)$, $C(\beta)$, $D(\beta)$, $G(\beta)$, and $H(\beta)$ are the matrices of adequate dimensions that describe the system and belong to a convex set of a polytopic nature given by

$$(A, B, C, D, H, G)(\beta) = \sum_{i=1}^{N} \beta_i (A, B, C, D, H, G)_i, \quad \beta \in \Lambda_p, \tag{3}$$

where N is given by the ratio $N = 2^\Phi$, where Φ denotes the number of distinct uncertain elements from the matrices (A, B, C, D, H, G), and $(A, B, C, D, H, G)_i$ represent the vertices of the polytope. Parameters β_i belong to a unit simplex Λ_p defined as

$$\Lambda_p = \left\{ \beta \in \mathbb{R}^N : \sum_{i=1}^{N} \beta_i = 1, \beta_i \geq 0, i \in \mathbb{K}_N \right\}. \tag{4}$$

Assuming that the state vector is available for feedback, we use the classical control law:

$$u(t) = -Kx(t). \tag{5}$$

Substituting (5) into the system (2) we have the following closed-loop system:

$$\dot{x}(t) = (A(\beta) - B(\beta)K)x(t) + H(\beta)w(t),$$
$$y(t) = (C(\beta) - D(\beta)K)x(t) + G(\beta)w(t). \tag{6}$$

Consider that the system (6) is excited by an exogenous input $w(t)$, with finite energy. The $\mathcal{H}_\infty$ norm establishes a limitation for the influence of the exogenous input $w(t)$ on the controlled output $y(t)$ [14]. It can be calculated as

$$\|H(s)\|_\infty = \max_{w\neq 0} \frac{\|y(t)\|_2}{\|w(t)\|_2}, \quad w(t) \in \mathscr{L}_2, \tag{7}$$

where $H(s)$ is the transfer function that relates output $y(t)$ and exogenous input $w(t)$ of the system.

The guaranteed cost $\mathcal{H}_\infty$ of the system is defined as the minimum value of γ, with $\gamma > 0$ and finite, such that

$$\|y(t)\|_2 < \gamma \, \|w(t)\|_2 \,, \tag{8}$$

wich means

$$\|H(s)\|_\infty < \gamma. \tag{9}$$

Consider the quadratic function of Lyapunov:

$$V(x) = x^T P x, \quad P = P^T > 0. \tag{10}$$

If the inequality (11) is true, then the stability of the feedback system (6) with the guaranteed cost $\mathcal{H}_\infty$ is ensured [15].

$$\dot{V}(x) + y^T y - \gamma^2 w^T w < 0. \tag{11}$$

In these terms, [15] presents the following theorem.

Theorem 1: [15] The system (1) - (2) with the control law (5) is asymptotically stable if, given a scalar $\mu > 0$, there are matrices $X = X^T > 0$ and M, of adequate size, satisfying the following optimization problem:

$$\begin{aligned} &min\ \mu \\ &s.a\ X = X^T > 0 \\ &\begin{bmatrix} He\{A_i X - B_i M\} & H_i & XC_i^T - M^T D_i^T \\ * & -\mu I & G_i^T \\ * & * & -I \end{bmatrix} < 0, \end{aligned} \tag{12}$$

for $i \in \mathbb{K}_N$ and $\gamma^2 = \mu > 0$. If (12) is feasible, then the feedback gain matrix is given by $K = MX^{-1}$, ensuring $\|H(s)\|_\infty < \sqrt{\mu}$.

Proof: See [15]. □

It is often necessary for the closed-loop eigenvalues of the system to be allocated within a particular region of interest, in order to ensure limits for some parameters, such as maximum overshoot, rise time and settling time. This region $S(\alpha, r, \theta)$ is defined in [13] and it uses the concept of $\mathcal{D}$-stability for the allocation of eigenvalues.

In this region $S(\alpha, r, \theta)$, that may be seen in Fig. 1, the complex eigenvalues of the system (in the form $x \pm jy$) satisfies

$$S(\alpha, r, \theta) = \begin{cases} x < -\alpha < 0, \\ |x \pm jy| < r, \\ \tan(\theta)x < -|y|. \end{cases} \tag{13}$$

The first constraint on (13) represents a half-plane to the left of the vertical line passing through the point $(-\alpha, 0)$, with $\alpha > 0$, the second constraint on (13) represents a disk of radius r centered at the origin and the third and last constraint of (13) limits the argument θ of the set elements.

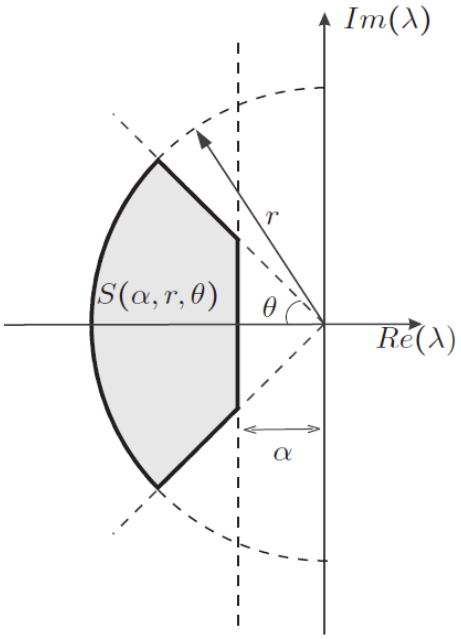

FIGURE 1. $S(\alpha, r, \theta)$ region for eigenvalues allocation.

In second order systems, the dynamic behavior of the system can be described in terms of two parameters: the damping coefficient and the undamped natural frequency [16]. When the eigenvalues of a second order system belong to the region $S(\alpha, r, \theta)$, the feedback system has minimal decay rate α, minimum damping coefficient $\zeta > \cos(\theta)$ and maximum damped frequency $\omega_d < r \sin(\theta)$ [13].

The following theorem, from [13], presents a condition sufficient to restrict the eigenvalues, in closed loop, in the region $S(\alpha, r, \theta)$.

Theorem 2: [13] The system (1) - (2) with the control law (5) has eigenvalues in the region $S(\alpha, r, \theta)$ if there exist matrices $X = X^T > 0$ and M, of appropriate dimensions, such that:

$$A_i X + X A_i^T - B_i M - M^T B_i^T + 2\alpha X < 0, \tag{14}$$

$$\begin{bmatrix} -rX & A_i X - B_i M \\ * & -rX \end{bmatrix} < 0, \tag{15}$$

$$\begin{bmatrix} \Gamma & \cos(\theta)(A_i X - X A_i^T - B_i M + M^T B_i^T) \\ * & \Gamma \end{bmatrix} < 0, \tag{16}$$

where $\Gamma = \sin(\theta)(A_i X + X A_i^T - B_i M - M^T B_i^T)$, $i \in \mathbb{K}_N$ and the feedback gain matrix is given by $K = MX^{-1}$.

Proof: See [13]. □

Remark 1: Note that the conditions presented in Theorems 1 and 2 allow the design of a robust $\mathcal{H}_\infty$ controller that uses a fixed gain to $\mathcal{D}$-stabilize the feedback system in the region $S(\alpha, r, \theta)$. These theorems will be useful to illustrate the applications of the main proposed results, for controlling an inverted pendulum system and an active suspension system, in Section V.

III. PROBLEM FORMULATION: THE POSITION-FEEDBACK CONTROL

For the first proposed method, a mechanical system is considered to have positions and velocities as state variables. However, although the design considers access to all plant state variables, the implementation considers access only to the position state variables for feedback.

Consider the following classical state space equation of a time-invariant linear mechanical system:

$$\dot{x}(t) = Ax(t) + Bu(t), \quad x(t) = [d(t)^T \ \dot{d}(t)^T]^T, \tag{17}$$

where $y(t) = d(t)$, $x \in \mathbb{R}^n$, $d \in \mathbb{R}^q$, $u \in \mathbb{R}^m$, $A \in \mathbb{R}^{n\times n}$ and $B \in \mathbb{R}^{n\times m}$, with $n = 2q$.

For the controller design initially consider the control law:

$$\dot{u}(t) = -[K_1 \ K_2 \ K_3] \begin{bmatrix} d(t) \\ \dot{d}(t) \\ u(t) \end{bmatrix}, \tag{18}$$

where $d(t)$ is the state vector of positions, $\dot{d}(t)$ is the state vector of velocities of the system, considering that both are available, and $K_1 \in \mathbb{R}^{m\times q}$, $K_2 \in \mathbb{R}^{m\times q}$ and $K_3 \in \mathbb{R}^{m\times m}$ are the controller gains. The closed loop system can be represented as:

$$\dot{x}_{tp}(t) = (A_{tp} - B_{tp}K_{tp})x_{tp}(t), \quad x_{tp}(t) = \begin{bmatrix} d(t) \\ \dot{d}(t) \\ u(t) \end{bmatrix}, \tag{19}$$

$$A_{tp} = \begin{bmatrix} A_{n\times n} & B_{n\times m} \\ 0_{m\times n} & 0_{m\times m} \end{bmatrix}, \quad B_{tp} = \begin{bmatrix} 0_{q\times m} \\ 0_{q\times m} \\ I_{m\times m} \end{bmatrix}, \tag{20}$$

$$K_{tp} = \begin{bmatrix} K_1 & K_2 & K_3 \end{bmatrix}. \tag{21}$$

With the closed-loop system introduced, the following theorem is proposed.

Theorem 3: If the plant (A, B) *presented in (17) is controllable, then* (A_{tp}, B_{tp}) *presented in (19) and (20) will also be controllable.*

Proof: Analyzing the system (19) controllability matrix, we have:

$$C = \begin{bmatrix} B_{tp} & A_{tp}B_{tp} & \cdots & A_{tp}^{n+m-1}B_{tp} \end{bmatrix},$$

$$C = \begin{bmatrix} 0 & B & AB & \cdots & A^{n-1}B & A^nB & \cdots & A^{n+m-1}B \\ I_m & 0 & 0 & \cdots & 0 & 0 & \cdots & 0 \end{bmatrix}. \tag{22}$$

Two new matrices are defined, then:

$$\mathbf{C_p} = \begin{bmatrix} B & AB & \cdots & A^{n-1}B \end{bmatrix}, \tag{23}$$

$$\mathbf{C_a} = \begin{bmatrix} A^nB & \cdots & A^{n+m-1}B \end{bmatrix}. \tag{24}$$

Note that the matrix $\mathbf{C_p} \in \mathbb{R}^{n\times(nm)}$ has rank n, because the original plant is controllable. Then:

$$\mathbf{C}\mathbf{C}^T = \begin{bmatrix} 0 & \mathbf{C_p} & \mathbf{C_a} \\ I_m & 0 & 0 \end{bmatrix} \begin{bmatrix} 0 & I_m \\ \mathbf{C_p}^T & 0 \\ \mathbf{C_a}^T & 0 \end{bmatrix},$$

$$\mathbf{C}\mathbf{C}^T = \begin{bmatrix} \mathbf{C_p}\mathbf{C_p}^T + \mathbf{C_a}\mathbf{C_a}^T & 0 \\ 0 & I_m \end{bmatrix}, \tag{25}$$

$$\mathbf{C}\mathbf{C}^T \geq \begin{bmatrix} \mathbf{C_p}\mathbf{C_p}^T & 0 \\ 0 & I_m \end{bmatrix} > 0, \tag{26}$$

since $rank(\mathbf{C_p}) = n$ and $\mathbf{C_p} \in \mathbb{R}^{n\times(nm)}$, so $\mathbf{C_p}\mathbf{C_p}^T > 0$. Besides $\mathbf{C_a}\mathbf{C_a}^T \geq 0$ for every $\mathbf{C_a} \in \mathbb{R}^{n\times m^2}$. Therefore, $\mathbf{C} \in \mathbb{R}^{(n+m)\times(n+m)m}$ has rank equal to $(n+m)$ and the augmented plant system (A_{tp}, B_{tp}) is controlable. □

Theorem 3 shows that the augmented system (19) and (20) is controllable, when the plant (17) is controllabe. It means that the introduction of the new state variables given by the vector u to the plant (17) to obtain the augmented system (19) and (20), does not add any conservatism in the controller design conditions for the plant.

Assuming, initially, that $x_{tp}(t)$ is available, a gain K_{tp} is designed so that the feedback system (19) shows adequate performance. This procedure can be done, for example, using techniques based on LMIs, considering several performance indices, such as: robustness, operating region, decay rate, among others. Next, consider the existence of $K_{tp} = [K_1 \ K_2 \ K_3] \in \mathbb{R}^{m\times(2q+m)}$ such that the controlled system presents a suitable performance. Observe that the initial conditon $u(0)$ can also be specified, if necessary. Then, note that the designed control law (18) can be represented as:

$$\begin{aligned} \int_0^t \dot{u}(t)dt &= u(t) - u(0) \\ &= \int_0^t (-K_1 d(t) - K_2\dot{d}(t) - K_3 u(t))dt \\ &= \int_0^t (-K_1 d(t) - K_3 u(t))dt + \int_0^t (-K_2\dot{d}(t))dt \\ &= \int_0^t (-K_1 d(t) - K_3 u(t))dt - K_2(d(t) - d(0)). \end{aligned} \tag{27}$$

Now, we define a function named $z(t)$ as:

$$z(t) = u(t) + K_2 d(t). \tag{28}$$

Thus, from (27) and (28) we have:

$$z(t) = \int_0^t (-K_1 d(t) - K_3 u(t))dt + u(0) + K_2 d(0), \tag{29}$$

$$z(0) = u(0) + K_2 d(0). \tag{30}$$

From (28)-(30) the control law (18) can be exactly represented by:

$$\dot{z}(t) = -K_1 d(t) - K_3 u(t), \tag{31}$$

$$u(t) = z(t) - K_2 d(t), \tag{32}$$

$$z(0) = u(0) + K_2 d(0). \tag{33}$$

Finally, substituting (32) into (31) it follows that:

$$\dot{z}(t) = (-K_1 + K_3K_2)d(t) - K_3 z(t). \tag{34}$$

Note that the control law $u(t)$ implemented as in (32) only uses $d(t)$ (the positions vector), not depending on $\dot{d}(t)$ (the velocities vector), and it is equivalent to the original control law (18), which considered both $d(t)$ and $\dot{d}(t)$ available.

In terms of block diagrams, Fig. 2 and Fig. 3 illustrate, respectively, the configurations used on the design and in the

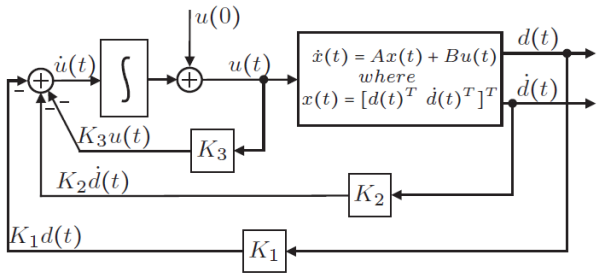

FIGURE 2. Initial illustration for the design with position-feedback.

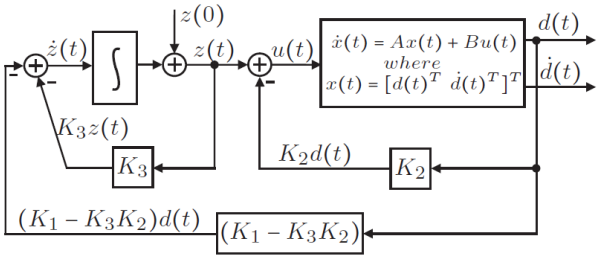

FIGURE 3. Implementation of the designed control system: Position-feedback.

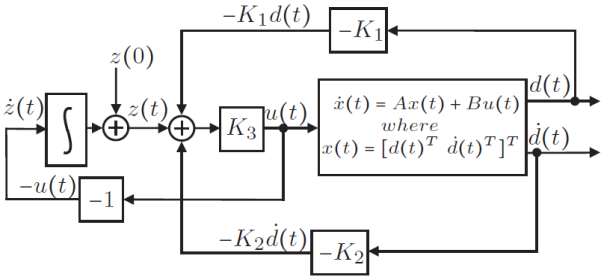

FIGURE 4. Initial illustration for the design with velocity-feedback.

implementation of the control law. The configuration in Fig. 2 is based on (17) and (18), while the configuration on Fig. 3, the implemented system, is determined by (17) and (32)-(34).

A possible disadvantage of the initial configuration shown in Fig. 2 is the use of the integrator to generate the control signal $u(t)$. This fact may make it difficult to obtain certain performance indices due to the fact that $u(t)$ can be seen as the area of the signal at the input of the integrator added to an initial condition $u(0)$.

The proper specification of $u(0)$ in Fig. 3 may improve this possible problem. For example, if $u(0) = -K_2 d(0)$, then we have that $z(0) = u(0) + K_2 d(0) = 0$ and, therefore, there exist only an initial condition vector that is different from zero in the system represented in Fig. 3, given by $x(0) = [d(0)^T \ \dot{d}(0)^T]^T$. Observe that this proposed control system is an interesting option for designing full state feedback for mechanical plants with uncertain parameters using only the feedback of the positions, considering that it is not needed to build an observer or similar to estimate the plant velocities. Furthermore, it is relatively cheaper because it is not necessary to measure the plant velocities, only the plant positions.

[10] designs an output feedback controller that does not need velocity measurements for its implementation and the structure of the proposed scheme consists of a proportional gain plus a dynamic gain resulting from a first-order system. On the present paper a different strategy is used to achieve a similar goal with the position-feedback control. In addition, the presence of polytopic uncertainties in the mechanical model used in the studies is considered in order to confirm the robustness of the designed controller.

IV. PROBLEM FORMULATION: THE VELOCITY-FEEDBACK CONTROL

The same classic system presented in (17) is considered, representing a mechanical system whose state variables are linked to positions and velocities. Once again, in the design stage it is considered that all state variables of the system are available for feedback. The new control law is presented in (35), being composed of three components: one related to position, one related to speed and another related to the integral of the control signal itself. The block diagram in Fig. 4 represents the initial design of the feedback system.

$$u(t) = -K_3[K_1 d(t) + K_2 \dot{d}(t) - \int_0^t u(t)dt - z(0)]. \quad (35)$$

Remark 2: A similarity to a PID (Proportional Integral Derivative Controller) is noticed in (35).

It is necessary, therefore, to end the direct dependence of the control signal on the state variables related to the positions ($d(t)$). For that, we have:

$$\int_0^t \dot{d}(t)dt = d(t) - d(0),$$
$$d(t) = \int_0^t \dot{d}(t)dt + d(0). \quad (36)$$

With this small maneuver it is possible to represent the system through another block diagram, presented in Fig 5 (where $g(0) = z(0) - K_1 d(0)$). The new diagram represents a system equivalent to the one presented in Fig. 4, with the important difference that the feedback is composed only by the velocity state variables.

From the original block diagram in Fig. 4, the following representation is made in the state space:

$$\dot{x}_{tv}(t) = A_{tv}x_{tv}(t) + B_{tv}u(t), \quad x_{tv}(t) = \begin{bmatrix} d(t) \\ \dot{d}(t) \\ z(t) \end{bmatrix}, \quad (37)$$

$$A_{tv} = \begin{bmatrix} A_{n\times n} & 0_{n\times m} \\ 0_{m\times n} & 0_{m\times m} \end{bmatrix}, \quad B_{tv} = \begin{bmatrix} B_{n\times m} \\ -I_{m\times m} \end{bmatrix}, \quad (38)$$

$$u(t) = K_3(-K_1 d(t) - K_2 \dot{d}(t) + z(t)),$$
$$= -\begin{bmatrix} K_3K_1 & K_3K_2 & -K_3 \end{bmatrix} \begin{bmatrix} d(t) \\ \dot{d}(t) \\ z(t) \end{bmatrix}, \quad (39)$$

$$= -\begin{bmatrix} K_3K_1 & K_3K_2 & -K_3 \end{bmatrix} \begin{bmatrix} \int_0^t \dot{d}(t)dt + d(0) \\ \dot{d}(t) \\ z(t) \end{bmatrix}. \quad (40)$$

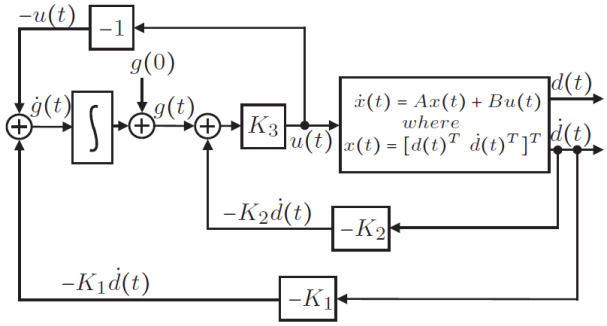

FIGURE 5. Implementation of the designed control system: Velocity-feedback.

It is noteworthy that the feedback gain vector, as presented in the control law (40), has the following format for a generic n-dimensional system:

$$K_{tv} = \begin{bmatrix} K_{n+1}K_1 & K_{n+1}K_2 & \cdots & K_{n+1}K_n & -K_{n+1} \end{bmatrix}. \quad (41)$$

Based on what was introduced, the following theorem is presented.

Theorem 4: If the plant (A, B) *presented in (17) is controllable and* $det(A) \neq 0$*, then* (A_{tv}, B_{tv}) *presented in (37) and (38) will also be controllable.*

Proof: Analyzing the system (37) controllability matrix, we have:

$$C = \begin{bmatrix} B_{tv} & A_{tv}B_{tv} & \cdots & A_{tv}^{n+m-1}B_{tv} \end{bmatrix},$$
$$C = \begin{bmatrix} B & AB & \cdots & A^{n-1}B & A^nB & \cdots & A^{n+m-1}B \\ -I_m & 0 & \cdots & 0 & 0 & \cdots & 0 \end{bmatrix}. \quad (42)$$

Two new matrices are defined, as described below:

$$\mathbf{C_p} = \begin{bmatrix} B & AB & \cdots & A^{n-1}B \end{bmatrix}, \quad (43)$$
$$\mathbf{C_a} = \begin{bmatrix} A^nB & \cdots & A^{n+m-1}B \end{bmatrix}. \quad (44)$$

Therefore, matrix $\mathbf{C}$ can be written as follows:

$$\mathbf{C} = \begin{bmatrix} \mathbf{C_p} & \mathbf{C_a} \\ [-I_m \ 0] & 0 \end{bmatrix}. \quad (45)$$

From (45) we have:

$$\mathbf{C}\mathbf{C}^T = \begin{bmatrix} \mathbf{C_p} & \mathbf{C_a} \\ [-I_m \ 0] & 0 \end{bmatrix} \begin{bmatrix} \mathbf{C_p}^T & \begin{bmatrix} -I_m \\ 0 \end{bmatrix} \\ \mathbf{C_a}^T & 0 \end{bmatrix}, \quad (46)$$

$$\mathbf{C}\mathbf{C}^T = \begin{bmatrix} \mathbf{C_p}\mathbf{C_p}^T + \mathbf{C_a}\mathbf{C_a}^T & \mathbf{C_p}\begin{bmatrix} -I_m \\ 0 \end{bmatrix} \\ [-I_m \ 0]\mathbf{C_p}^T & I_m \end{bmatrix}. \quad (47)$$

Applying the Schur complement [15] to (47) it is possible to affirm that $\mathbf{C}\mathbf{C}^T > 0$ if and only if:

$$\mathbf{C_p}\mathbf{C_p}^T + \mathbf{C_a}\mathbf{C_a}^T - \mathbf{C_p}\begin{bmatrix} -I_m \\ 0 \end{bmatrix} I_m [-I_m \ 0]\mathbf{C_p}^T > 0, \quad (48)$$

$$[\mathbf{C_p} \ \mathbf{C_a}] \begin{bmatrix} \mathbf{C_p}^T \\ \mathbf{C_a}^T \end{bmatrix} - \mathbf{C_p} \begin{bmatrix} I_m & 0 \\ 0 & 0 \end{bmatrix} \mathbf{C_p}^T > 0. \quad (49)$$

Calculating the second term in (49), from (43) it follows that:

$$\mathbf{C_p} \begin{bmatrix} I_m & 0 \\ 0 & 0 \end{bmatrix} \mathbf{C_p}^T = BB^T. \quad (50)$$

Substituting (50), (43) and (44) in (49) one obtains:

$$[B \ AB \ \cdots \ A^{n+m-1}B][B^T \ (AB)^T \ \cdots \ (A^{n+m-1}B)^T]^T - BB^T > 0,$$
$$[AB \ \cdots \ A^{n+m-1}B][(AB)^T \ \cdots \ (A^{n+m-1}B)^T]^T > 0. \quad (51)$$

Using a mathematical artifice, matrix A is put in evidence to the left of the first term and matrix A^T is put in evidence to the right of the second term of (51). Thus, we have:

$$A[B \ AB \ \cdots \ A^{n+m-2}B][B^T \ (AB)^T \ \cdots \ \cdots \ (A^{n+m-2}B)^T]^T A^T > 0. \quad (52)$$

Therefore, from (43) and defining

$$\mathbf{C_a^-} = [A^nB \, A^{n+1}B \cdots A^{n+m-2}B],$$

it follows that:

$$A[\mathbf{C_p} \ \mathbf{C_a^-}] \begin{bmatrix} \mathbf{C_p}^T \\ \mathbf{C_a^-}^T \end{bmatrix} A^T = A(\mathbf{C_p}\mathbf{C_p}^T + \mathbf{C_a^-}\mathbf{C_a^-}^T)A^T, \quad (53)$$

$$A(\mathbf{C_p}\mathbf{C_p}^T + \mathbf{C_a^-}\mathbf{C_a^-}^T)A^T \geq \mathbf{C_p}\mathbf{C_p}^T > 0, \quad (54)$$

because $\mathbf{C_p} \in \mathbb{R}^{n\times(n+m)}$ and A have rank n, bearing in mind that the original plant (A, B) is controllable and $det(A) \neq 0$. Thus, the controllability of the plant for the augmented system (A_{tv}, B_{tv}) is maintained. □

Remark 3: If $det(A) = 0$*, then the plant (17) cannot be stabilizable when only* $\dot{y}(t) = \dot{d}(t)$ *is available for feedback [17].*

Remark 4: The proposed procedures for controlling mechanical systems, using only the feedback of all positions or only the feedback of all velocities, can be classified as output feedback controls, since usually the state variables of mechanical systems are the positions and the velocities. However, an important additional characteristic of these new control implementations is that they allow the design of controllers considering full access to the state variables of the plant. The implementation of these controller structures, consider m additional integrators, where m is the number of the plant inputs, as described in Figures 3 and 5.

Remark 5: Note that in the proposed procedures, the number of inputs (m) *and the rank of the input matrix* $B(\beta)$ *of the plant given in (1) and (2) can be arbitrary and are not related to the number of plant state variables* (n)*. Thus, they can be applied in many situations, for instance, in the implementation of controllers for underactuated and also fully-actuated systems. The implementation of controllers for nonlinear systems with these new methods is a topic for future researches.*

V. SIMULATION RESULTS

Some examples of mechanical systems are presented along with several simulations results to prove the effectiveness of the proposed method. The simulations were performed using the Simulink tool of the MATLAB software.

At first the inverted pendulum system is presented, which is a simpler case. Later the active suspension system, which is the focus of this paper and, therefore, also had practical results collected and presented in the paper.

In order to design a controller that guarantees adequate system performance and, also, that can be implemented in practice, some values were determined empirically for parameters related to the $S(\alpha, r, \theta)$ region, after a series of multivalued tests for these parameters.

A. INVERTED PENDULUM SYSTEM

Consider the inverted pendulum model shown in Fig. 6. The mass of the pendulum (m) is concentrated at its tip and its length is l. A variable torque $\tau(t)$ is applied to the pendulum at the position of its articulation to keep it balanced with the 0 radian angle. $\phi(t)$ represents the inclination angle of the pendulum and g denotes the gravity acceleration. The system dynamics are given by:

$$ml^2\ddot{\phi}(t) + mgl\sin\phi(t) = \tau(t). \tag{55}$$

Linearizing the system model around the equilibrium point $(\phi_0, \dot{\phi}_0) = (0, 0)$, described in the form of state space, we have:

$$\dot{x}(t) = \begin{bmatrix} 0 & 1 \\ -\dfrac{g}{l} & 0 \end{bmatrix} x(t) + \begin{bmatrix} 0 \\ \dfrac{1}{ml^2} \end{bmatrix} u(t), \tag{56}$$

$$x(t) = \begin{bmatrix} \phi(t) \\ \dot{\phi}(t) \end{bmatrix}, \quad u(t) = \tau(t). \tag{57}$$

Remark 6: The linearized model allows a first illustration of the possibility of applying the proposed method, considering that the linearized model is widely used in control designs when the feedback system operates in regions close to the equilibrium point. When the state variables are far away from the equilibrium point, the control performance of inverted pendulums may be influenced by the terms neglected in the linearization process and present an inadequate performance.

For the simulations related to the inverted pendulum, the following values were adopted for the system parameters: $m = 0.1$kg, $l = 0.5$m and $g = 9.8$m/s^2. However, a polytopic uncertainty is considered for for the pendulum mass, with a variation of $\pm 10\%$, representing that m could vary from 0.09 to 0.11kg. Therefore, the vertices of the polytope on the control design are presented on (58).

$$A_1 = A_2 = \begin{bmatrix} 0 & 1 \\ -19.6000 & 0 \end{bmatrix},$$
$$B_1 = \begin{bmatrix} 0 \\ 36.3636 \end{bmatrix}, \quad B_2 = \begin{bmatrix} 0 \\ 44.4444 \end{bmatrix}. \tag{58}$$

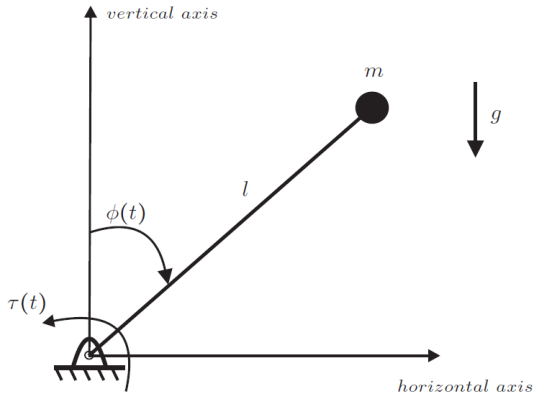

FIGURE 6. Schematic model of the inverted pendulum system.

1) INVERTED PENDULUM SYSTEM - POSITION FEEDBACK

For the simulation, after a series of tests, the α parameter was delimited in '2' and r in '40', while θ had no restriction. Solving the LMIs presented in Theorem 2 using the values mentioned for α and r and considering (18)-(21), the following parameters were obtained:

$$P = \begin{bmatrix} 0.0821 & 0.0025 & 0.0018 \\ 0.0025 & 0.0001 & 0.0001 \\ 0.0018 & 0.0001 & 0.0001 \end{bmatrix},$$
$$K_{tp} = \begin{bmatrix} 778.1146 & 50.2633 & 62.2170 \end{bmatrix}. \tag{59}$$

The inverted pendulum linearized model was used for the controller design folowing the structure described in Fig. 2. However, the results of the simulations presented are from the controller applied to the real, nonlinearized model, using only the feedback of the position and following the procedure given in Fig. 3. On Fig. 7 and Fig. 8, it is possible to see the angle and angular velocity variation over time, respectively. On Fig. 9 it is shown the controlled input signal. The pendulum bar initially has a tilt angle of $\pi/4$ rad (45°), as shown in Fig. 7. Analyzing Figs. 7-9 we can see that the feedback system was able to stabilize in less than 4 seconds. Therefore, the effectiveness of the limited feedback for the first example is proved.

2) INVERTED PENDULUM SYSTEM - VELOCITY FEEDBACK

Considering the same inverted pendulum model (Fig. 6), new simulations were performed with the velocity feedback method. The α parameter was delimited in '0.3' and r in '40', while θ had once again no restriction. Solving the LMIs presented in Theorem 2, we obtain:

$$P = \begin{bmatrix} 0.1979 & 0.0019 & -0.3080 \\ 0.0019 & 0.0021 & 0.0610 \\ -0.3080 & 0.0610 & 3.0725 \end{bmatrix},$$
$$K_{tv} = \begin{bmatrix} 7.1160 & 0.4215 & -11.2841 \end{bmatrix}. \tag{60}$$

The design was based on the block diagram given in Fig. 4. The implementation of the controller uses only the feedback of the velocity, following the structure presented in Fig. 5 with the plant represented by its nonlinear model (55). The

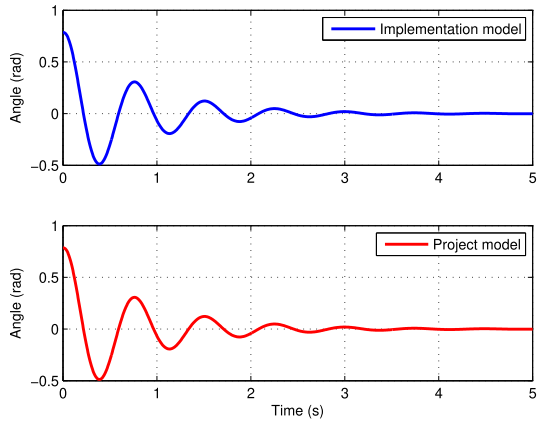

FIGURE 7. Angle variation on inverted pendulum simulation - position feedback.

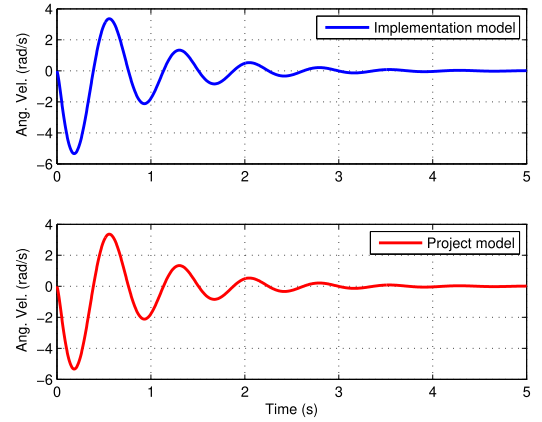

FIGURE 8. Angular velocity variation on inverted pendulum simulation - position feedback.

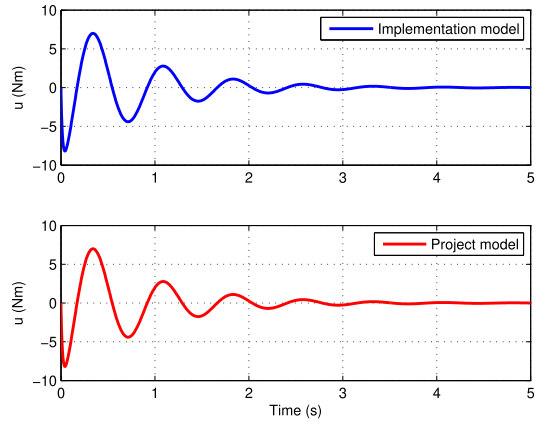

FIGURE 9. Controlled input signal on inverted pendulum simulation - position feedback.

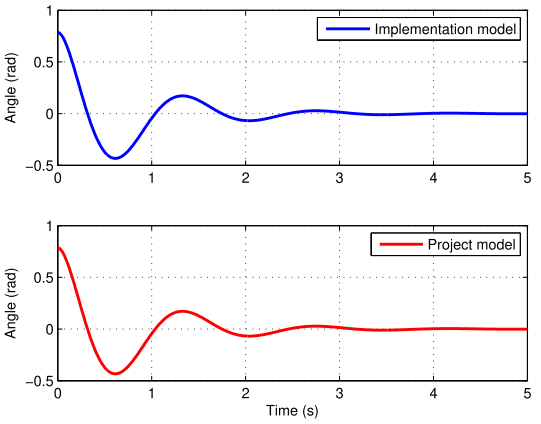

FIGURE 10. Angle variation on inverted pendulum simulation - velocity feedback.

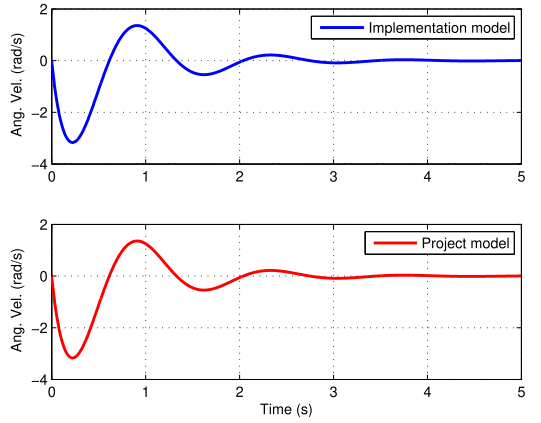

FIGURE 11. Angular velocity variation on inverted pendulum simulation - velocity feedback.

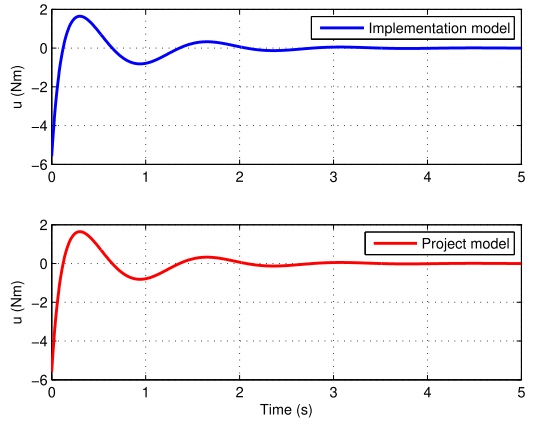

FIGURE 12. Controlled input signal on inverted pendulum simulation - velocity feedback.

angle and angular velocity variation over time are presented on Fig. 10 and Fig. 11, respectively, while the controlled input signal is presented on Fig. 12. Again, the initial angle of the pendulum bar is $\pi/4$ rad (45°).

The velocity-feedback system was able to stabilize even faster than the position-feedback system, in addition to having a less oscillatory transient. So, the effectiveness of the limited feedback is verified once again.

B. QUANSER ACTIVE SUSPENSION SYSTEM

Consider the didactic active suspension system of a vehicle manufactured by Quanser® that can be seen in Fig. 13 [11], [18]. The schematic model with more details is represented in Fig. 14. The system consists of a set of two masses, called by M_s and M_{us}. The M_s mass represents a portion of the total vehicle body ($\frac{1}{4}$ if the vehicle is a car or $\frac{1}{2}$ if it is a motorcycle, for example) and is supported by the spring k_s

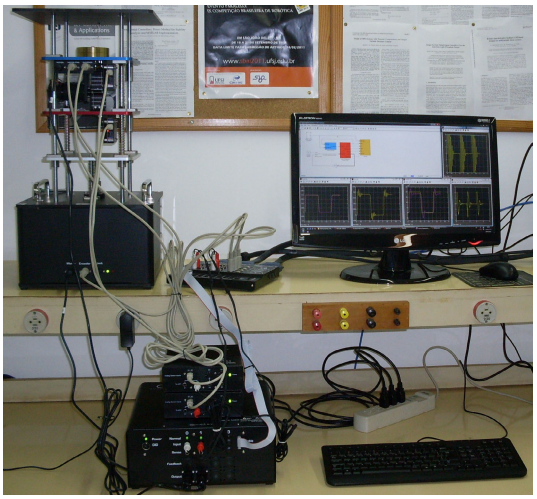

FIGURE 13. Active suspension system from quanser® belonging to the LPC-FEIS-UNESP (Brazil).

and by the damper b_s. The M_{us} mass corresponds the mass of the tire set and is supported by the spring k_{us} and by the damper b_{us}. The vibrations caused by irregularities in the street can be attenuated by the vehicle's active suspension system, represented by a motor (actuator) connected between the masses M_s and M_{us}, and controlled by the force F_c [14]. The dynamic model of the Quanser Active Suspension [11] can be represented in the form of state space in (61)-(62).

$$\dot{x}(t) = \begin{bmatrix} 0 & 0 & 1 & -1 \\ 0 & 0 & 0 & 1 \\ -\frac{k_s}{M_s} & 0 & -\frac{b_s}{M_s} & \frac{b_s}{M_s} \\ \frac{k_s}{M_{us}} & -\frac{k_{us}}{M_{us}} & \frac{b_s}{M_{us}} & -\frac{(b_s+b_{us})}{M_{us}} \end{bmatrix} x(t) + \begin{bmatrix} 0 \\ 0 \\ \frac{1}{M_s} \\ -\frac{1}{M_{us}} \end{bmatrix} u(t) + \begin{bmatrix} 0 \\ -1 \\ 0 \\ \frac{b_{us}}{M_{us}} \end{bmatrix} w(t), \tag{61}$$

with

$$x(t) = \begin{bmatrix} z_s(t) - z_{us}(t) \\ z_{us}(t) - z_r(t) \\ \dot{z}_s(t) \\ \dot{z}_{us}(t) \end{bmatrix} \quad and \quad w(t) = \dot{z}_r(t). \tag{62}$$

The positions $z_s(t)$, $z_{us}(t)$ and $z_r(t)$ are measured by encoders and the values for the system parameters are presented on Table 1. The presence of polytopic uncertainties in the active suspension system was considered for carrying out control designs, with the uncertainties relating to the mass of the vehicle body portion M_s (values ranging between 1.455 and 2.45 kg). Some papers, like [19], use acceleration measurements for the control method of the Quanser active suspension system, but for the methods proposed on this paper these measurements are not necessary.

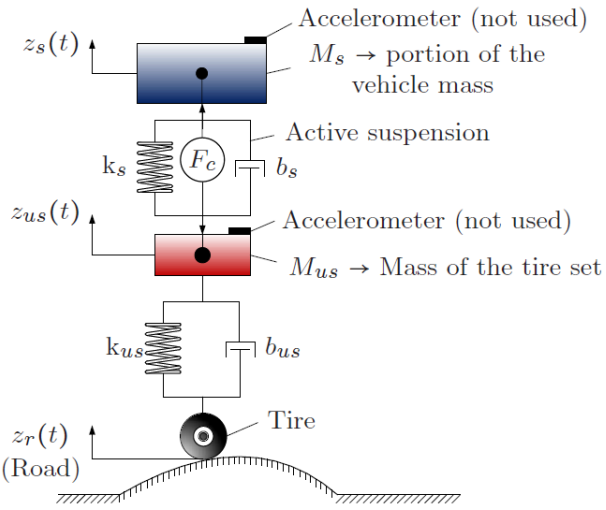

FIGURE 14. Schematic model of the active suspension system.

TABLE 1. Parameters of the active suspension system.

Parameters	Symbol	Value
Mass of part of vehicle body (kg)	M_s	1.455 - 2.450
Mass of the tire set (kg)	M_{us}	1
Stiffness constant of the spring (N/m)	k_s	900
Stiffness constant of the spring (N/m)	k_{us}	2500
Damping coefficient (Ns/m)	b_s	7.5
Damping coefficient (Ns/m)	b_{us}	5

Substituting the values presented in Table 1, considering the polytopic uncertainties, we have the following local models for the vertices of the polytope:

$$A_1 = \begin{bmatrix} 0 & 0 & 1 & -1 \\ 0 & 0 & 0 & 1 \\ -618.6 & 0 & -5.2 & 5.2 \\ 900 & -2500 & 7.5 & -12.5 \end{bmatrix},$$

$$A_2 = \begin{bmatrix} 0 & 0 & 1 & -1 \\ 0 & 0 & 0 & 1 \\ -367.3 & 0 & -3.1 & 3.1 \\ 900 & -2500 & 7.5 & -12.5 \end{bmatrix},$$

$$B_1 = \begin{bmatrix} 0 \\ 0.7 \\ 0 \\ -1 \end{bmatrix}, \quad B_2 = \begin{bmatrix} 0 \\ 0.4 \\ 0 \\ -1 \end{bmatrix},$$

$$H_1 = H_2 = \begin{bmatrix} 0 \\ 0 \\ -1 \\ 5 \end{bmatrix}. \tag{63}$$

1) ACTIVE SUSPENSION - POSITION FEEDBACK

For the active suspension system simulation working with the position feedback, α was delimited in '8' and r in '48', while θ had no restriction. Solving the LMIs presented in Theorems 1 and 2 using the aforementioned values for α and r, the following parameters were obtained as (64), shown at the bottom of the next page.

The design was based on the block diagram given in Fig. 2. The implementation of the controller uses only the feedback

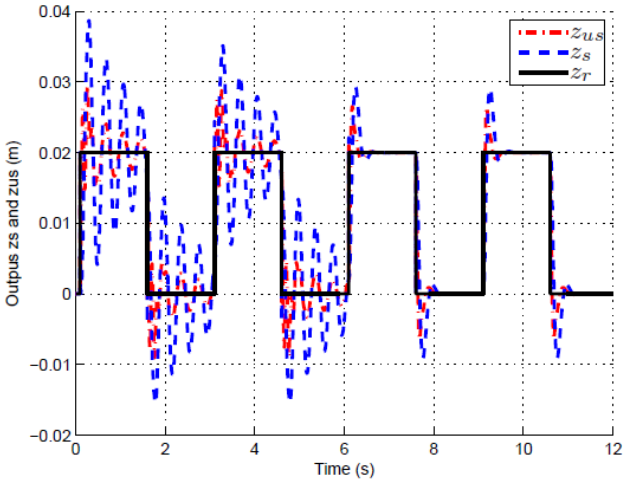

FIGURE 15. System outputs and track profile on active suspension simulation - position feedback.

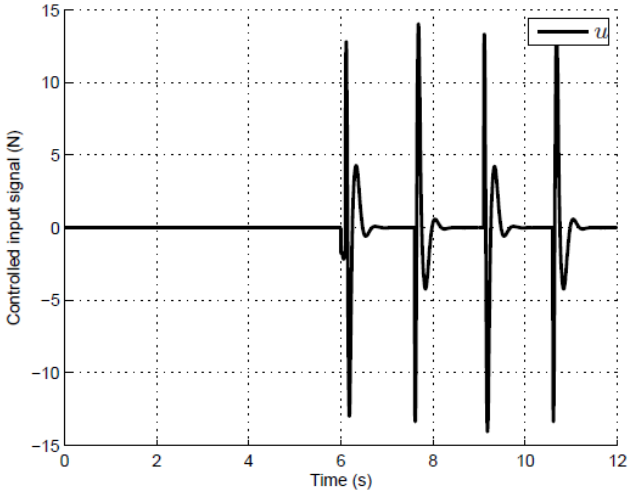

FIGURE 16. Controlled input signal on active suspension simulation - position feedback.

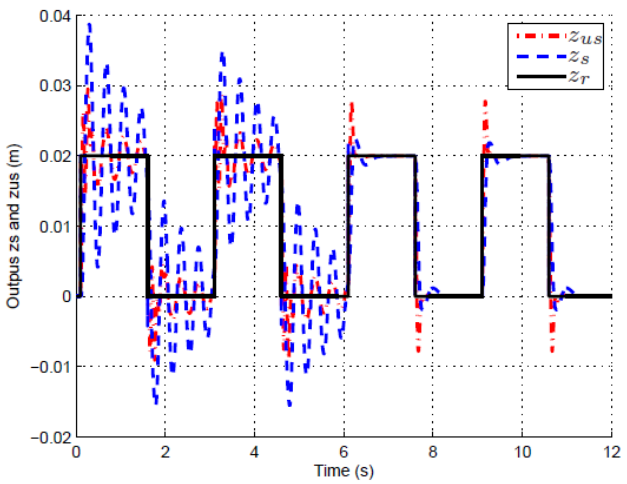

FIGURE 17. System outputs and track profile on active suspension simulation - velocity feedback.

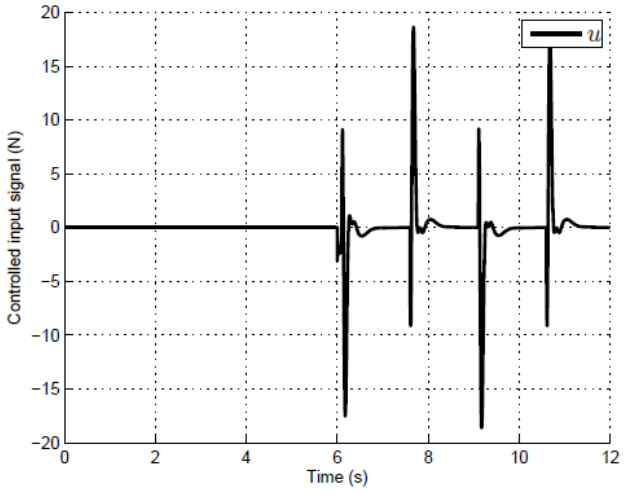

FIGURE 18. Controlled input signal on active suspension simulation - velocity feedback.

of the positions, following the structure presented in Fig. 3 with the plant (61) and (62) represented as an uncertain linear time-invariant system described in (1)-(4).

In the simulation that generated Fig. 15 and Fig. 16 a square wave signal with amplitude of 0.02 meters is simulated in the track profile. It is possible to observe in Fig. 15 the vertical displacement of the vehicle (z_s), of the tire set (z_{us}), besides the own track profile (z_r). On the time interval of 0 to 6 seconds the system is in open loop, while from 6 seconds onwards the system starts to work in closed loop using the designed controller (only position feedback).

The controlled input signal of the simulated system is shown in Fig. 16. Clearly, this input has zero value until the instant of 6 seconds, due to the fact that the system is working in an open loop mode. On the closed loop system, the controlled input reaches a maximum value of approximately 14 N

$$
\begin{aligned}
P &= \begin{bmatrix} 0.2860 & -0.1615 & -0.0042 & 0.0062 & -0.0003 \\ -0.1615 & 0.5389 & 0.0036 & -0.0026 & 0.0003 \\ -0.0042 & 0.0036 & 0.0017 & -0.0006 & 0.0000 \\ 0.0062 & -0.0026 & -0.0006 & 0.0004 & -0.0000 \\ -0.0003 & 0.0003 & 0.0000 & -0.0000 & 0.0000 \end{bmatrix}, \\
K_{tp} &= 10^4 \times \begin{bmatrix} -4.4522 & 5.6958 & 0.1018 & 0.0560 & 0.0072 \end{bmatrix}, \\
&\|H(s)\|_\infty \leq \gamma = \sqrt{\mu} = 0.1429. \qquad (64)
\end{aligned}
$$

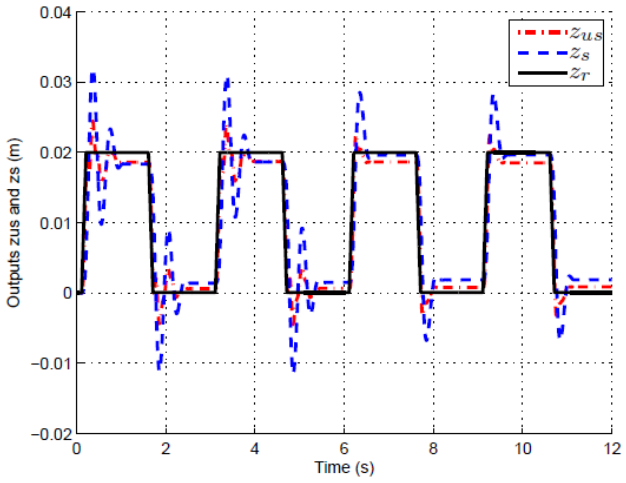

FIGURE 19. System outputs and track profile on active suspension implementation - position feedback.

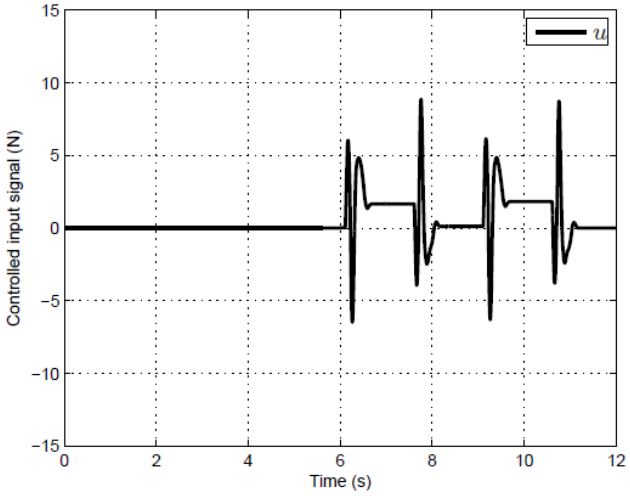

FIGURE 20. Controlled input signal on active suspension implementation - position feedback.

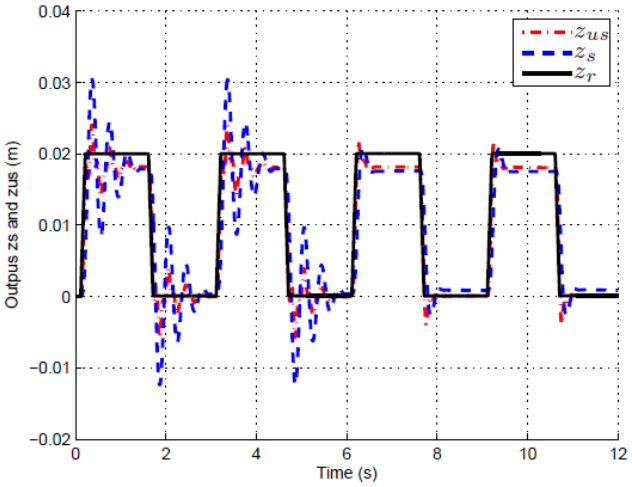

FIGURE 21. System outputs and track profile on active suspension implementation - velocity feedback.

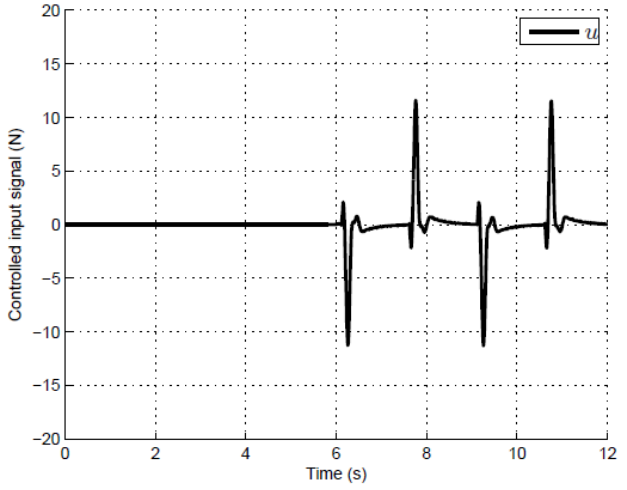

FIGURE 22. Controlled input signal on active suspension implementation - velocity feedback.

on the simulation, wich is a perfectly acceptable value for the practical implementation of the project ($\pm 39.2\ N$).

2) ACTIVE SUSPENSION - VELOCITY FEEDBACK

For the active suspension system simulation working with the velocity feedback, α was delimited in '6' and r in '45', while θ again had no restriction. Solving the LMIs presented in Theorems 1 and 2 the following parameters were obtained as (65), shown at the bottom of the page.

The design was based on the block diagram given in Fig. 4. The implementation of the controller uses only the feedback of the velocities, following the structure presented in Fig. 5 with the plant (61) and (62) represented as an uncertain linear time-invariant system described in (1)-(4).

The simulations conducted in this stage had the same conditions as for the system with position feedback in terms of initial conditions and track profile. The vertical displacement of the vehicle (z_s), of the tire set (z_{us}) and the track profile

$$
\begin{aligned}
P &= \begin{bmatrix} 168.9295 & 7.8169 & 5.5849 & -0.3403 & -1.3279 \\ 7.8169 & 196.0425 & -3.2073 & 1.7824 & -0.2172 \\ 5.5849 & -3.2073 & 0.3192 & -0.0446 & -0.0357 \\ -0.3403 & 1.7824 & -0.0446 & 0.0737 & 0.0020 \\ -1.3279 & -0.2172 & -0.0357 & 0.0020 & 0.0123 \end{bmatrix}, \\
K_{tv} &= \begin{bmatrix} -223.8343 & 384.0248 & 42.6896 & -25.8383 & -2.7703 \end{bmatrix}, \\
&\|H(s)\|_\infty \leq \gamma = \sqrt{\mu} = 2.8111.
\end{aligned} \tag{65}
$$

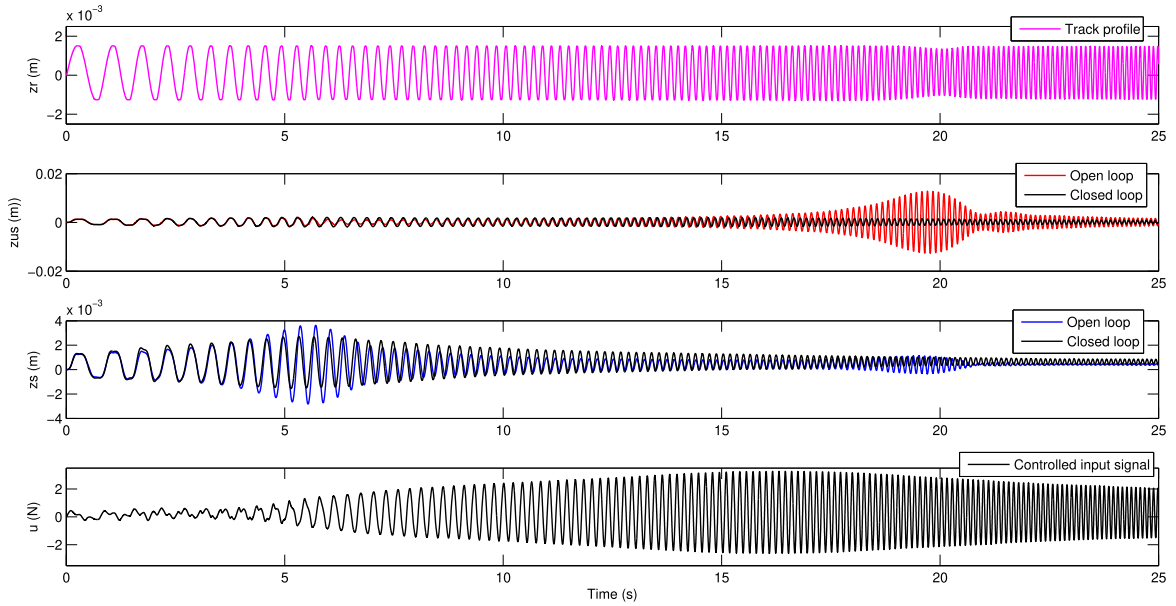

FIGURE 23. Active suspension system response for a increasing frequency on the track profile - position feedback.

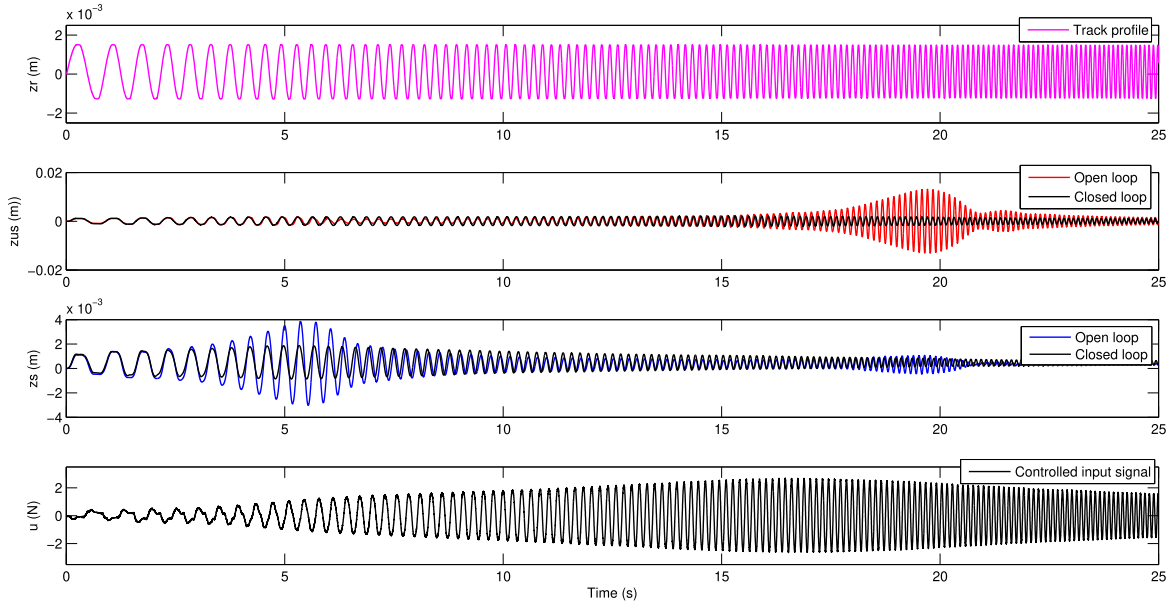

FIGURE 24. Active suspension system response for a increasing frequency on the track profile - velocity feedback.

(z_r) are presented in Fig. 17, while the controlled input signal of the simulated system is shown in Fig. 18. The velocity feedback system has a similar performance to the position feedback system, showing a slightly better performance considering the peak of z_s in the transient for the closed loop system. On the other hand, the controlled input signal peaks showed higher values, but still, far from the practical limits of the system.

VI. PRACTICAL IMPLEMENTATION FOR ACTIVE SUSPENSION SYSTEM

In this section the practical results for the active suspension system are presented. The same conditions simulated on computer for this system were implemented in laboratory with the two methods presented: position and velocity feedback.

A. LABORATORY RESULTS - POSITION FEEDBACK

On Fig. 19 we have once again z_s, z_{us} and z_r, as showed on Fig. 15, with similar results. Some challenges are to reduce the transitory peak and the steady state error.

It is presented in Fig. 23 the system behavior (open loop and closed loop) when the track profile is a variable frequency sinusoid, ranging from 1 to 10 Hertz in 25 seconds. This experiment was carried out in order to demonstrate the

ability of the feedback system to cancel the resonant frequencies present in the open loop system. Clearly, the control method does a great job of nullifying the resonance around 20 seconds.

B. LABORATORY RESULTS - VELOCITY FEEDBACK

On Fig. 21 are presented z_s, z_{us} and z_r, showing similar results to Fig. 17. For this case a smoother transient can be observed than for the position feedback method.

The controlled input signal is presented in Fig. 22, showing slightly higher values than the practical results for the controlled input signal in the system with position feedback, just like it was observed on the simulations.

The active suspension system is once again put under the influence of a track profile composed of a variable frequency sinusoid, just like it was done for the position feedback method. The results are presented on Fig. 24, proving the velocity feedback method is also capable of canceling the resonant frequency in the open loop system.

VII. CONCLUSION

In this paper, the design of a control signal that depends only on part of the system state variables is the main characteristic. A set of LMIs was used to achieve stability and adequate performance. It was verified that, despite the limitation in the feedback of the system, both control methods (position and velocity feedback) worked satisfactorily for the examples presented. For the active suspension system, there was an overshoot even with the closed loop system, especially for the system with position feedback, while the case with speed feedback showed a very small overshoot peak. Therefore, the proposed control systems are interesting options for the design and implementation of full state feedback for plants with uncertain parameters using only output feedback (only positions feedback or only velocities feedback), considering that it is not needed to build an observer to estimate any plant state variable. Furthermore, they are relatively cheaper because it is not necessary to measure all state variables of the plant. Some next steps for the research are the possibility working with switched state-feedback control and designing a hybrid control method, which works with partial access to position state variables and partial access to the velocity ones.

REFERENCES

[1] P. Gahinet, A. Nemirovski, A. J. Laub, and M. Chilali, *LMI Control Toolbox for Use With MATLAB*, The MathWorks, Natick, MA, USA, 1995.
[2] D. Shin, W. Kim, Y. Lee, and C. C. Chung, "Nonlinear position control for permanent magnet stepper motor using only position feedback," in *Proc. 13th Int. Conf. Control, Autom. Syst. (ICCAS)*, Gwangju, South Korea, Oct. 2013, pp. 11–16.
[3] C. Guerrero, V. Santibanez, Y. Araiza-Olvera, E. Ibarra-Figueroa, and B. Perez-Perez, "Control of velocity of DC motors by classical and passivity methods measuring only position: Theory and experimental comparison," *IEEE Latin Amer. Trans.*, vol. 18, no. 5, pp. 962–970, May 2020.
[4] S. Avila-Becerril, A. Loria, and E. Panteley, "Global position-feedback tracking control of flexible-joint robots," in *Proc. Amer. Control Conf. (ACC)*, Boston, MA, USA, Jul. 2016, pp. 3008–3013.
[5] J. Faigl and P. Čížek, "Adaptive locomotion control of hexapod walking robot for traversing rough terrains with position feedback only," *Robot. Auto. Syst.*, vol. 116, pp. 136–147, Jun. 2019.
[6] A.-C. Huang and C.-T. Huang, "FAT-based robot adaptive control with position measurements only," in *Proc. Chin. Control Decis. Conf. (CCDC)*, Nanchang, China, Jun. 2019, pp. 3516–3520.
[7] F. A. Salam, "Velocity feedback control and the dynamic properties of robot manipulators," in *Proc. 26th IEEE Conf. Decis. Control*, Los Angeles, CA, USA, Dec. 1987, pp. 2217–2220.
[8] H. Li, H. Liu, and H. Gao, "Robust quantised control for active suspension systems," *IET Control Theory Appl.*, vol. 5, no. 17, pp. 1955–1969, Nov. 2011.
[9] W. Sun, H. Pan, J. Yu, and H. Gao, "Reliability control for uncertain half-car active suspension systems with possible actuator faults," *IET Control Theory Appl.*, vol. 8, no. 9, pp. 746–754, 2014.
[10] R. Rascón and J. Moreno-Valenzuela, "Output feedback controller for trajectory tracking of robot manipulators without velocity measurements nor observers," *IET Control Theory Appl.*, vol. 14, no. 14, pp. 1819–1827, Sep. 2020.
[11] *Active Suspension System—User Manual*, Quanser Innovate Educate, Adv. Mechtron. Collection, ON, Canada, 2009.
[12] J. Löfberg, "YALMIP: A toolbox for modeling and optimization in MATLAB," in *Proc. IEEE Int. Conf. Robot. Automat.*, Taipei, Taiwan, Sep. 2004, pp. 284–289.
[13] M. Chilali and P. Gahinet, "H_∞ design with pole placement constraints: An LMI approach," *IEEE Trans. Autom. Control*, vol. 41, no. 3, pp. 358–367, Mar. 1996.
[14] D. R. de Oliveira, M. C. M. Teixeira, U. N. L. T. Alves, W. A. de Souza, E. Assunção, and R. Cardim, "On local H_∞ switched controller design for uncertain T–S fuzzy systems subject to actuator saturation with unknown membership functions," *Fuzzy Sets Syst.*, vol. 344, pp. 1–26, Aug. 2018.
[15] S. Boyd, L. El Ghaoui, E. Feron, and V. Balakrishnan, *Linear Matrix Inequalities in System and Control Theory*, vol. 15. Philadelphia, PA, USA: SIAM, 1994.
[16] K. Ogata, *Modern Control Engineering*, 5th ed. Upper Saddle River, NJ, USA: Prentice-Hall, 2010.
[17] M. R. Moreira, E. I. M. Júnior, T. T. Esteves, M. C. M. Teixeira, R. Cardim, E. Assunção, and F. A. Faria, "Stabilizability and disturbance rejection with state-derivative feedback," *Math. Problems Eng.*, vol. 2010, Dec. 2010, Art. no. 123751.
[18] E. R. P. da Silva, E. Assunção, M. C. M. Teixeira, and R. Cardim, "Robust controller implementation via state-derivative feedback in an active suspension system subjected to fault," in *Proc. Conf. Control Fault-Tolerant Syst. (SysTol)*, Nice, FR, Oct. 2013, pp. 752–757.
[19] S. D. Garcia and D. Patino, "Estimation based on acceleration measures of an active suspension plant," in *Proc. IEEE 2nd Colombian Conf. Autom. Control (CCAC)*, Manizales, CO, USA, Oct. 2015, pp. 284–289.

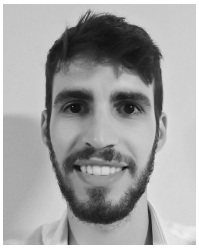

LUCAS M. ESTEVES was born in Jaú, Brazil, in 1989. He received the B.Sc., M.Sc., and D.Sc. degrees in electrical engineering from Universidade Estadual Paulista (UNESP), Ilha Solteira, Brazil, in 2014, 2017, and 2020, respectively. From 2016 to 2017, he worked as a Substitute Professor with the Federal Institute of Education, Science and Technology of São Paulo. His research interests include control theory and its applications, linear matrix inequalities-based designs, variable structure control, sliding modes control, and switched systems.

RODRIGO CARDIM was born in Adamantina, Brazil, in 1981. He received the B.Sc. degree in electrical engineering from São Paulo State University (UNESP), Ilha Solteira, Brazil, in 2004, and the Ph.D. degree, in 2009. In 2012, he held a postdoctoral position. He is currently a Professor with the Department of Electrical Engineering, UNESP. His research interests include control theory and applications, linear matrix inequalities-based designs, variable structure control, fuzzy systems, and switched systems. He received the São Paulo Engineering Institute Award for the Best Undergraduate Student of the year 2004 at UNESP.

MARCELO C. M. TEIXEIRA (Member, IEEE) was born in Campo Grande, Brazil, in 1957. He received the B.Sc. degree in electrical engineering from the Escola de Engenharia de Lins, Lins, Brazil, in 1979, the M.Sc. degree in electrical engineering from the Instituto Alberto Luiz Coimbra de Pós-graduação e Pesquisa de Engenharia, Universidade Federal do Rio de Janeiro, Rio de Janeiro, Brazil, in 1982, and the D.Sc. degree in electrical engineering from the Pontifícia Universidade Católica do Rio de Janeiro, Rio de Janeiro, in 1989. In 1982, he joined the Department of Electrical Engineering, Universidade Estadual Paulista (UNESP), Ilha Solteira (FEIS), Brazil, where he is currently a Professor. In 1996 and 1997, he was a Visiting Scholar with the School of Electrical and Computer Engineering, Purdue University,West Lafayette, IN, USA. He was a Coordinator, from 1991 to 1993, and a Vice Coordinator, from 1989 to 1991, and from 1993 to 1995, of the undergraduate program in electrical engineering with FEIS-UNESP, where he was a Coordinator, from 2005 to 2007, and a Vice Coordinator, from 2000 to 2005, and from 2007 to 2010, of the postgraduate program in electrical engineering. His research interests include control theory and applications, neural networks, variable-structure systems, linear-matrix-inequality-based designs, fuzzy systems, nonlinear systems, adaptive systems, and switched systems. From 2009 to 2013, he was a member of the Brazilian Evaluation Committee of Postgraduate Courses IV Engineering CAPES. From 2016 to 2020, he was an Associate Editor of the IEEE TRANSACTIONS ON FUZZY SYSTEMS.

DIOGO R. DE OLIVEIRA was born in Andradina, Brazil, in 1990. He received the B.Sc. degree in electrical engineering from São Paulo State University (UNESP), Ilha Solteira, Brazil, in 2012, and the Ph.D. degree, in 2017. In 2020, he held a postdoctoral position at UNESP. In 2017, he joined the Federal Institute of Education, Science and Technology of Mato Grosso do Sul (IFMS), Campus Três Lagoas, Brazil, where he is currently a Professor. His research interests include control theory and applications, linear matrix inequalities-based designs, switched systems, $\mathcal{H}_\infty$ control, and fuzzy systems.

JEAN M. DE S. RIBEIRO received the B.Sc., M.Sc., and D.Sc. degrees in electrical engineering from Universidade Estadual Paulista (UNESP), Ilha Solteira, Brazil, in 1998, 2001, and 2006, respectively. He is currently an Assistant Professor with the Department of Electrical Engineering, UNESP. His research interests include control theory and its applications, variable structure control, sliding modes control, and the control and electronic drive of electrical machines.

EDVALDO ASSUNÇÃO was born in Andradina, Brazil, in 1965. He received the B.Sc. degree from São Paulo State University (UNESP), Ilha Solteira, Brazil, in 1989, the M.Sc. degree from the Instituto Tecnológico de Aeronáutica, Brazil, in 1991, and the D.Sc. degree from the Universidade Estadual de Campinas, Brazil, in 2000, all in electrical engineering. In 1992, he joined the Department of Electrical Engineering, UNESP, where he is currently an Assistant Professor. His research interests include control theory and applications, linear matrix inequalities-based design, optimal, and robust control. He received the Instituto de Engenharia de São Paulo Award from FEIS-UNESP, in 1989.

HYAGO R. M. SILVA was born in Frutal, Brazil, in 1994. He received the B.Sc. and M.Sc. degrees in electrical engineering from São Paulo State University (UNESP), Ilha Solteira, Brazil, in 2018 and 2020, respectively. He is currently a Doctoral Student with the Department of Electrical Engineering, UNESP, and a Substitute Professor with the Department of Electrical Engineering, Federal Institute of Education, Science and Technology of São Paulo. His research interests include control theory and applications, linear matrix inequalities-based designs, fuzzy systems, and switched systems. He received the São Paulo Engineering Institute Award from FEIS-UNESP for the Best Undergraduate Student of the year 2018.